JOURNAL OF NATURAL PRODUCTS

Article

pubs.acs.org/jnp

Methoxyflavones from *Stachys glutinosa* with Binding Affinity to Opioid Receptors: In Silico, in Vitro, and in Vivo Studies

Stefania Ruiu,[†,▽] Nicola Anzani,[‡,▽] Alessandro Orrù,[†] Costantino Floris,[§] Pierluigi Caboni,[⊥] Stefano Alcaro,[∥] Elias Maccioni,[‡] Simona Distinto,[‡] and Filippo Cottiglia*[,‡]

[†]Institute of Translational Pharmacology, UOS of Cagliari, National Research Council, Parco Scientifico e Tecnologico, Pula, Cagliari, Italy

[‡]Department of Life and Environmental Sciences, Drug Sciences Section, University of Cagliari, Via Ospedale 72, 09124 Cagliari, Italy

[§]Dipartimento di Scienze Chimiche, University of Cagliari, Complesso di Monserrato, Monserrato, 09042, Italy

[⊥]Department of Life and Environmental Sciences, High Resolution Mass Spectrometry Laboratory, University of Cagliari, Via Ospedale 72, 09124 Cagliari, Italy

[∥]Dipartimento di Scienze della Salute, Università "Magna Græcia" di Catanzaro, Campus "S. Venuta", Viale Europa, 88100 Catanzaro, Italy

Supporting Information

ABSTRACT: Fractionation of the bioactive dichloromethane extract from the aerial parts of *Stachys glutinosa* led to the isolation of four flavones, xanthomicrol (**1**), sideritoflavone (**2**), 8-methoxycirsilineol (**3**), and eupatilin (**4**), along with two *neo*-clerodane diterpenes, roseostachenone (**8**) and a new compound, 3α,4α-epoxyroseostachenol (**7**). In order to study structure−activity relationships, two methoxyflavones [5-demethyltangeretin (**5**) and tangeretin (**6**)] were synthesized by the methoxylation of xanthomicrol. The isolated compounds (**1**−**4**, **7**, and **8**) as well as the xanthomicrol semisynthetic derivatives (**5** and **6**) were evaluated for their binding affinity to the μ and δ opioid receptors. Xanthomicrol was the most potent binder to both μ and δ receptors, with a K_i value of 0.83 and 3.6 μM, respectively. Xanthomicrol administered intraperitoneally in mice at a dose of 80 mg/kg significantly reduced morphine-induced antinociception in the tail flick test. Our results suggested that xanthomicrol is a μ opioid receptor antagonist. Docking experiments were carried out to acquire a deeper understanding about important structural aspects of binding of xanthomicrol. In summary, these data suggest that xanthomicrol is a valuable structure for further development into a potential μ opioid receptor antagonist.

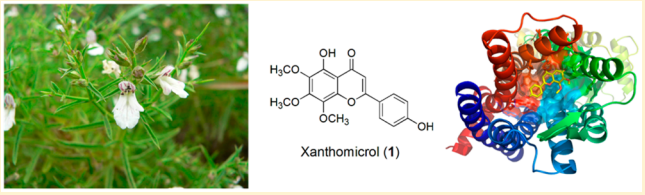

Flavonoids are secondary metabolites widely distributed in higher plants that show various biological properties including antioxidative, anti-inflammatory, estrogenic, antiviral, anticarcinogenic, and cardioprotective activities.[1] Flavonoids are also present in edible fruits and vegetables, and many experimental studies support the potential utility of dietary flavonoids in the treatment of many diseases.[2] Unfortunately, the most promising dietary flavonoids such as quercetin, chrisin, kaempferol, and apigenin have very low bioavailability, making them largely ineffective *in vivo*.[3−5] The poor bioavailability is due either to limited absorption or to extensive metabolism. In fact such compounds are polyhydroxylated flavonoids (PHFs), and the free hydroxyl groups limit the intestinal absorption and are quickly conjugated by glucuronidation and sulfation.[6,7] On the contrary, polymethoxylated flavonoids (PMFs) are readily absorbed in the intestine and show wide tissue distribution and metabolic stability.[6,8] Various PMFs have been identified in edible plants such as in citrus fruits,[9−11] pepper vine leaves,[12] and also propolis.[13] Thus, PMF_S may be more biologically active dietary flavonoids compared to their hydroxylated analogues.

Continuing our search for opioid ligands from Sardinian native plants,[14] we have found that the CH_2Cl_2 extract obtained from the aerial parts of *Stachys glutinosa* L. (Lamiaceae) exhibited substantial binding affinity for μ and δ opioid receptors (MOR and DOR). This study aimed first to identify the bioactive metabolites of the CH_2Cl_2 extract and evaluate their binding affinity to opioid receptors and, second, to assess whether the most potent opioid binder was able to exert antinociceptive action in mice. *S. glutinosa* is an endemic shrub of Sardinia, Corsica, and Capraia Islands that grows on different substrata.[15] The plant is used in Sardinian folk medicine as an antispasmodic and antiseptic.[16] Because of the unpleasant and strong balsamic smell, the plant is employed as an antifeedant against chicken lice.[17]

RESULTS AND DISCUSSION

The powered dried aerial parts of *S. glutinosa* were percolated with CH_2Cl_2. The CH_2Cl_2 extract exhibited good binding affinity

Received: September 11, 2014

DOI: 10.1021/np500671v
J. Nat. Prod. XXXX, XXX, XXX−XXX

to μ and δ opioid receptors (Table 1) and was therefore subjected to fractionation by silica gel vacuum-liquid chromatography (VLC) and column chromatography (silica gel and Sephadex LH 20) to give one new *neo*-clerodane (**7**) along with four known flavones (**1**–**4**) and one known *neo*-clerodane (**8**).

Table 1. K_i Values of the CH_2Cl_2 Extract and Isolated Compounds for Opioid Receptors[a]

	receptor affinity (μM)		MOR selectivity
compd	K_i(MOR)	K_i(DOR)	K_i(DOR)/K_i(MOR)
CH_2Cl_2	10.3 ± 0.2[b]	9.0 ± 1[b]	0.87:1
1	0.83 ± 0.02	3.6 ± 0.8	4.36:1
2	18.5 ± 0.8	12.5 ± 1	0.68:1
3	>50	37.5 ± 4	
4	28.0 ± 0.4	12.0 ± 2	0.43:1
5	>50	>50	
6	16.3 ± 1.5	7.0 ± 0.5	0.43:1
7	>50	25.0 ± 0.9	
8	40.5 ± 7.5	23.5 ± 0.5	0.58:1

[a] K_i values were obtained from four independent experiments carried out in triplicate and are expressed as mean ± standard error. [b] Values expressed in μg/mL.

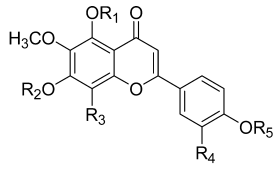

1 R_1 = H; R_2 = CH_3; R_3 = OCH_3; R_4 = H; R_5 = H
2 R_1 = H; R_2 = CH_3; R_3 = OCH_3; R_4 = OH; R_5 = H
3 R_1 = H; R_2 = CH_3; R_3 = OCH_3; R_4 = OCH_3; R_5 = H
4 R_1 = H; R_2 = H; R_3 = H; R_4 = OCH_3; R_5 = CH_3
5 R_1 = H; R_2 = CH_3; R_3 = OCH_3; R_4 = H; R_5 = CH_3
6 R_1 = CH_3; R_2 = CH_3; R_3 = OCH_3; R_4 = H; R_5 = CH_3

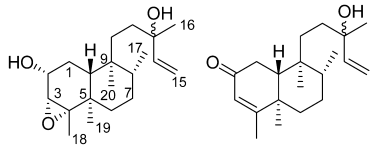

Compound **7** was obtained as a white, amorphous solid. The ^{13}C NMR spectrum of compound **7** exhibited 20 carbon signals, which were sorted by APT NMR into five CH_3, six CH_2, five CH, and four quaternary carbons. These data were in agreement with the molecular formula $C_{20}H_{34}O_3$ and consistent with the measured pseudomolecular ion at m/z 345.2418 $[M + Na]^+$ (calcd 345.2406) in HRTOFESIMS. The ^{1}H NMR spectrum of **7** revealed four methyl groups at δ_H 0.66 (3H, s, H_3-20), 1.04 (3H, s, H_3-19), 1.20 (3H, s, H_3-18), and 1.28 (3H, s, H_3-16), one secondary methyl group at δ_H 0.76 (3H, d, J = 6.5 Hz, H_3-17), a vinyl system (δ_H 5.08, 1H, dd, J = 1, 10.8 Hz, H-15a; 5.21, 1H, dd, J = 1, 17.2 Hz, H-15b; 5.88, 1H, dd, J = 10.8, 17.2 Hz, H-14), two oxygenated methine protons at δ_H 3.06 (1H, br s, H-3) and 3.90 (1H, ddd, J = 2.0, 6.0 Hz, H-2), two methines at δ_H 0.88 (1H, br d, J = 11.5 Hz) and 1.42 (1H, m, H-8), and a partially overlapped resonance due to five methylenes from δ_H 1.16 to δ_H 1.65. The ^{1}H and ^{13}C NMR spectra of **7** were very similar to those of the *neo*-clerodane diterpene roseostachenone (**8**). The main differences between the two compounds were the presence of two oxymethines at δ_H 3.90 (δ_C 70.7) and 3.06 (δ_C 65.2) instead of a ketone group (δ_C 200.5) and of an olefinic proton signal at δ_H 5.67 (δ_C 125.5) in roseostachenone. The observed HMBC correlations of the oxymethine at δ_H 3.06 with C-1 (δ_C 25.3), C-2 (δ_C 70.7), C-4 (δ_C 70.4), and C-18 (δ_C 19.4), of the further oxymethine at δ_H 3.90 with C-1 and C-3 (δ_C 65.2), and of methylene protons at δ_H 1.63 and 1.16 with C-2, C-3, C-5 (δ_C 36.2), and C-10 (δ_C 46.3) (Figure 1) suggested that the two

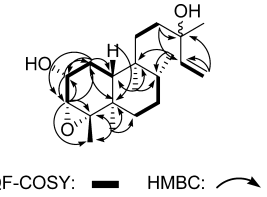

Figure 1. Main HMBC and DQF-COSY correlations of compound **7**.

oxymethine protons at δ_H 3.90 and 3.06 were attached to C-2 and C-3, respectively. The location of the above-mentioned protons was confirmed by DQF-COSY experiments. In fact, in the COSY spectrum the proton at δ_H 3.90 correlated with the methine at δ_H 3.06 and with the methylene protons at δ_H 1.63 and 1.16, while the methine at 3.06 ppm showed cross-peaks with the proton at 3.90 but not with those at 1.63 and 1.16 ppm (Figure 1).

Since compound **7** had 4° of unsaturation, **7** could also contain one epoxide ring. This hypothesis was confirmed by the presence of a broad singlet at δ_H 3.06 (H-3) in the ^{1}H NMR spectrum, indicating a 3,4-epoxy group. The relative configuration of **7** was elucidated analyzing the ^{13}C NMR values and by a ROESY experiment. The chemical shifts of C-19 and C-20 clearly indicated a trans-AB ring junction.[18] ROE cross-peaks of H-2/H-10, H-1β/H-2, and H-2/H-3 were congruent with an α-orientation for both the C-2 hydroxyl group and 3,4-epoxy group (Figure 2). Thus, the structure of compound **7** is 3α,4α-epoxyroseostachenol.

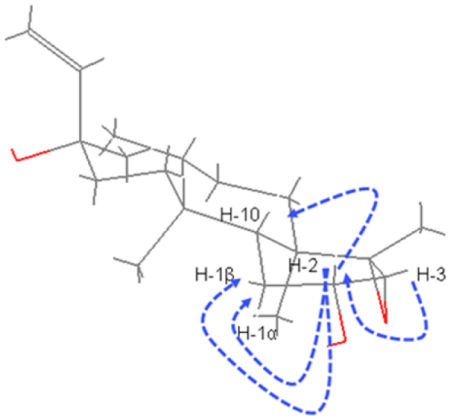

Figure 2. Key ROE correlations observed for compound **7**.

The structure of the known compounds were identified comparing the spectral and physical data with those reported in the literature, namely, xanthomicrol (**1**),[19] sideritoflavone (**2**),[20] 8-methoxycirsilineol (**3**),[21] eupatilin (**4**),[22] and roseostachenone (**8**).[23]

In order to gain information on the structure–activity relationship, two key derivatives, 5-demethyltangeretin (**5**) and tangeretin (**6**), were also prepared by methylation with dimethyl sulfate of xanthomicrol hydroxyl groups. The analytical and

DOI: 10.1021/np500671v
J. Nat. Prod. XXXX, XXX, XXX–XXX

spectroscopic data of **5** and **6** were identical to those reported in the literature.[10,24,25]

The CH_2Cl_2 extract from *S. glutinosa* exhibited an interesting binding affinity for MOR and DOR with K_i values of 10.3 and 9.0 μg/mL, respectively (Table 1). Among the isolated compounds, xanthomicrol (**1**) displayed the strongest opioid binding affinity to both μ and δ opioid receptors (K_i for MOR = 0.83 μM, K_i for DOR = 3.6 μM). Moreover, it showed the highest MOR selectivity with a ratio K_i(DOR)/K_i(MOR) = 4.4. The presence of a further hydroxy group at the 3′ position, as in sideritoflavone (**2**), significantly reduced the binding affinity for MOR (K_i = 18.5 μM), while the replacement of this group with a methoxy moiety, as in 8-methoxycirsilineol (**3**), abolished the affinity for MOR (K_i > 50 μM). In the semisynthetic derivative of compound **1**, 5-demethyltangeretin (**5**), the 4′-hydroxy group has been substituted with a methoxy moiety. This substitution had a dramatic effect on MOR with respect to compound **1**. 5-Demethyltangeretin had no significant affinity for MOR (K_i > 50 μM). When both the free hydroxy groups of compound **1** were methoxylated, as in tangeretin (**6**), the affinity for MOR was 20-fold lower than that of **1**. Taken together, these results suggested that, for a high affinity to MOR, 5-hydroxy-6,7,8-trimethoxy-flavones should be substituted with only one free hydroxyl group at the 4′ position of the B ring. The *neo*-clerodanes **7** and **8** exhibited very low affinity to μ and δ receptors.

To evaluate the pharmacological effect of the most potent methoxyflavone, **1**, the antinociceptive effect of xanthomicrol was assayed in an animal model of acute pain (tail-flick test). Figure 3 shows the effects of xanthomicrol (40 and 80 mg/kg, body wt ip) pretreatment on morphine-induced analgesia in the tail-flick test, carried out in mice. Xanthomicrol alone was devoid of analgesic activity in the tail-flick test. Morphine alone, at a dose of 5 mg/kg, increased the tail-flick latency 60 min after its administration [$F_{treatment}(1.37) = 33.63$, $p < 0.0001$; $F_{treatment\times time}(2.74) = 6.83$, $p < 0.005$; Tukey's test, $p < 0.05$ vs vehicle + saline-treated mice]. Xanthomicrol pretreatment, at a dose of 80 mg/kg, completely suppressed the analgesic effect of morphine [$F_{pretreatment}(2.37) = 7.51$, $p < 0.005$; $F_{pretreatment\times treatment}(2.37) = 3.61$, $p < 0.05$; $F_{pretreatment\times time}(4.74) = 1.09$, $p = 0.37$; $F_{pretreatment\times treatment\times time}(4.74) = 0.52$, $p = 0.72$]. On the contrary, 40 mg/kg of xanthomicrol failed to reduce the analgesic activity of morphine (Tukey's test, $p < 0.05$ vs vehicle + saline-treated mice).

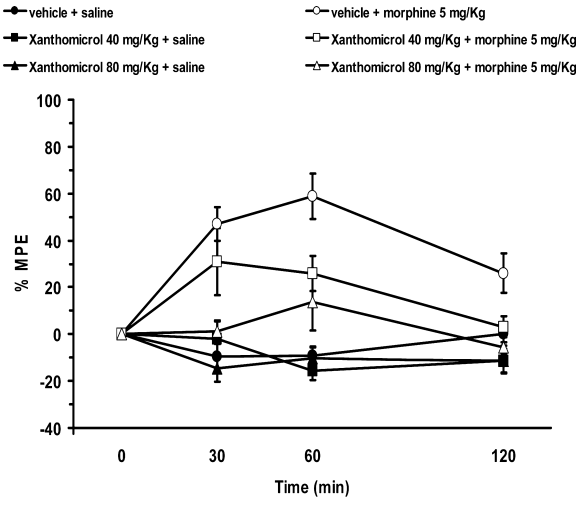

Figure 3. Effect of xanthomicrol pretreatment on morphine-induced analgesia in the tail-flick test. Saline or xanthomicrol (40 and 80 mg/kg, ip) were administered 30 min before 5 mg/kg, sc morphine injection. Basal algesia was assessed immediately prior to saline or xanthomicrol pretreatment (baseline). The effects of the drugs were evaluated 30, 60, and 120 min after morphine treatment. (See Experimental Section for further details.) Results are expressed as % MPE. Each point represents the mean ± SEM of 3−11 mice per group. *$p < 0.05$ vs vehicle + saline-treated mice (three-way ANOVA followed by Tukey's post hoc test).

Docking experiments were carried out to predict the xanthomicrol (**1**) binding orientation in order to gain a deeper understanding of the key structural aspects of binding. In this respect, it was decided to apply a consensus docking approach: applying four individual molecular docking algorithms and clustering the best poses of the most active ligand (**1**). Therefore, four programs were considered: Glide,[26] FLAPdock,[27,28] AutoDock,[29] and AutoDock Vina.[30] Most docking algorithms are able to locate molecules according to experimental observations (X-ray or NMR data); however their performance depends on the target.[31] In order to validate the docking protocols, β-funaltrexamine (β-FNA) was docked. This compound is a selective covalent inhibitor of G-protein-coupled μ-opioid receptor (MOR), recently cocrystallized and available in PDB with accession code 4DKL.[32] The docking protocols are described in the Experimental Section. Redocking poses were compared to the crystallographic pose using the root-mean-square deviation (RMSD) calculation method. As expected, the instances of docking experiments occur for a flexible portion of the molecule (4-oxo-2-butenoicacid methyl ester). Figure 4 shows a comparison of the binding mode predicted with the different programs and the bound ligand observed in the crystallographic structure. The linkage occurrence between a ligand and its receptor can be geometrically favored if they form a stable Michealis−Menten complex with their reactive moieties compatible with the formation of a covalent bond. This concept was successfully applied predicting the best poses of reactive epoxide against purine of duplex DNA.[33] Therefore, docking programs should be able to reproduce a conformation of the ligand before covalent binding. In this respect FLAPDock resulted as the best. However, all programs successfully reproduced the β-FNA core portion bound conformation (i.e., molecule without a flexible chain, Figure 4).

In addition, the electron density maps observed with Coot[34] highlighted a positive density of the F_o-F_c map (i.e., parts of the electron density not represented in the model (in green) that superimposed with the chain conformation retrieved by the other programs. Moreover, the terminal portion of the chain was not less defined by the $2F_o-F_c$ map (in blue) than the rest. This may be explained by the flexibility of the ligand chain and the Lys233$^{5.39}$ residue. In light of these results, all four considered programs can be efficiently used in order to investigate the key structural aspects of binding this target.

Hence, regular docking was performed considering the best compound (**1**) with a semiflexible protocol, retaining the protein as a rigid structure and the ligand as flexible. However, it is well known that protein flexibility plays an important role in the protein−ligand-induced fit process. Hence the obtained [**1**·μ-OR] complexes were subjected to a postdocking procedure based on energy minimization, leaving the residues around the ligand free to move and keeping the rest fixed, since the receptor is embedded in the membrane.

The analysis of docking experiment results obtained by the four docking programs revealed a consensus of two alternative binding conformations (Figure 5). These finding were plausible

DOI: 10.1021/np500671v
J. Nat. Prod. XXXX, XXX, XXX−XXX

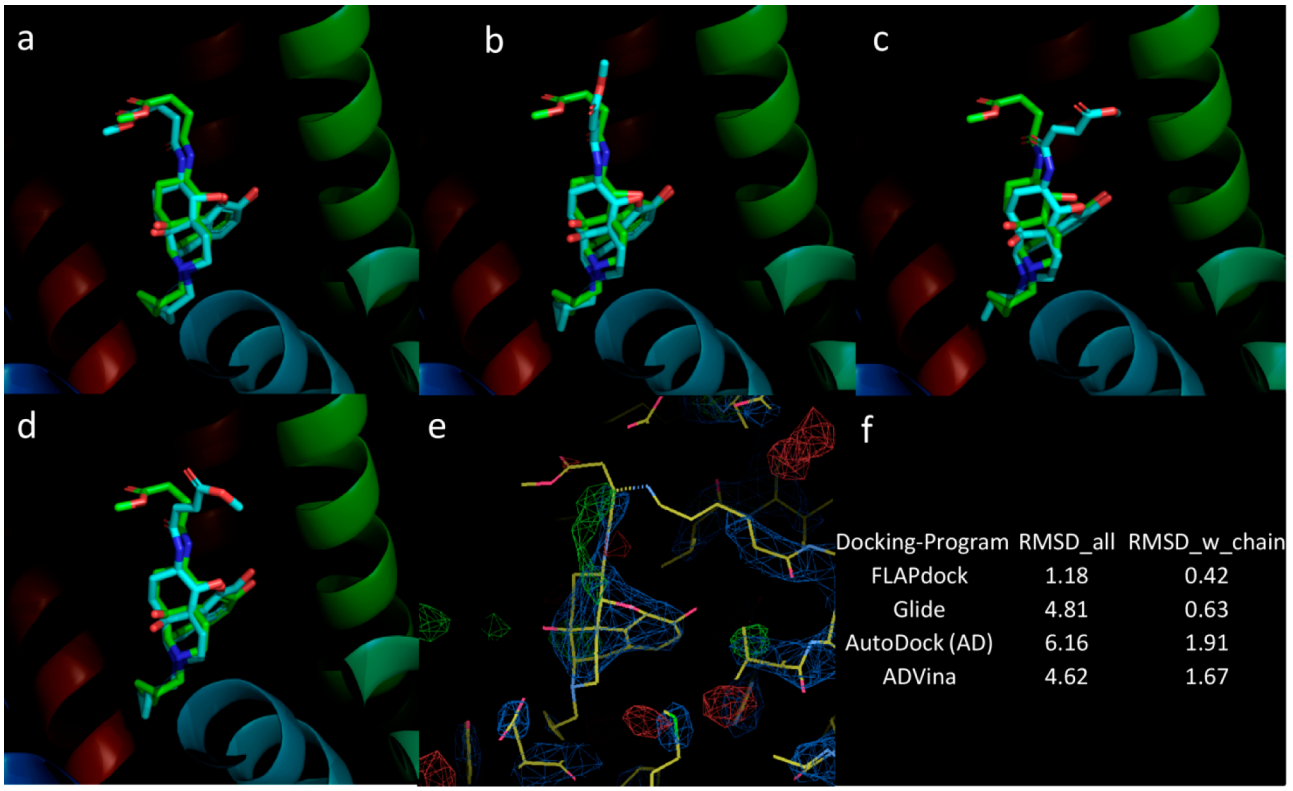

Figure 4. Redocking results (in cyan) compared to the crystallographic pose (in green) obtained by four docking programs: (a) FLAPdock, (b) Glide, (c) AutoDock, and (d) ADVina; (e) electron density maps of 4DKL visualized in Coot; (f) RMSD between crystallized and docked poses: all atoms and without 2-butenoic acid methyl ester portion.

since the binding pocket of μ-OR was wide compared with ligand size. Both binding modes were stabilized by an array of hydrogen bonds (HBs), aromatic interactions, and hydrophobic interactions between the molecule and the residues in the binding cavity. In particular, the OH-phenyl portion was entangled in a cavity, while the flavone moiety was stabilized by hydrophobic residues around the open cavity. The key role of the hydroxyl group in the para position of the phenyl ring was clear. In fact, in both binding modes, establishing a HB interaction with Gly325$^{7.42}$ helped the stabilization of the complex in the former and with His297$^{6.52}$ in the latter. The phenyl ring, instead, had a $\pi-\pi$ stacking interaction with Trp293$^{6.48}$ and His297$^{6.52}$, respectively. In addition a HB could be observed that involved the hydroxyl group in position 5 of the flavones and Cα-Ile296$^{6.51}$, in the first binding mode, and with Tyr326$^{7.43}$, in the second (Figure 5). The 4′OH-phenyl group was located in a shallow cavity, which could badly accommodate a second substituent in the meta position due to steric hindrance. This could explain the lower activity of compounds **2**, **3**, and **4**. At the same time, the lack of biological activity following substitution of the 4′-hydroxyl group also could be due to an analogous reason (e.g., compounds **4**, **5**, and **6**), and it would imply the loss of an important HB. The crucial role of the 4′OH-phenyl group was also demonstrated by the analysis of GRID maps,[35,27] since this portion fitted the energetically favorable areas highlighted by DRY (hydrophobic) and N1 (donor) probes. This analysis supported also the hypothesis of the double binding mode, as both binding poses well matched with MIF maps (Figure 6). Moreover the maps could be helpful to guide the lead structure optimization.

The results showed that xanthomicrol, the main constituent of *S. glutinosa* aerial parts (2% of the dried extract), was the principal responsible for the observed binding affinities of the extract. Among all the tested PMFs, xanthomicrol presented the highest binding inhibition of the selective tritiated ligand [^{3}H]DAMGO to MOR, with a K_i value of 0.83 μM. Structure−activity relationship studies and in silico studies indicated that the presence of only one free hydroxyl group at the 4′ position of the B ring seems to be important for a high affinity of 5-hydroxy-6,7,8-trimethoxyflavones to MOR. Since MOR is thought to be primarily responsible for the mediation of opioid antinociception, the antinociceptive activity of xanthomicrol in the tail-flick test has been evaluated. It was demonstrated that pretreatment with xanthomicrol inhibited morphine-induced antinociception in the tail-flick test, suggesting an antagonistic effect at MOR.

Despite the large amounts of articles reporting on the pharmacological activities of flavonoids, relatively few studies on the opioid receptors' binding affinity of these compounds have been reported.[36−40] In some works it has been demonstrated that the antinociceptive effect exerted by flavonoids in mouse thermal models of nociception was related to the activation of the opioid receptors.[36,41−44] Although some hydroxyflavones have been identified as opioid antagonists,[39] none have been shown to inhibit morphine-induced antinociception in an animal model of acute pain. As far as we know, we reported for the first time that a flavone administered intraperitoneally in mice significantly reduced morphine-induced antinociception in a dose-dependent manner in the tail-flick test and that, in all probability, its action is mediated, at least in part, by opioid receptors. Previous studies reported that xanthomicrol is moderately cytotoxic against cancer cells and has a low cytotoxicity against normal cells.[45] Meckes et al.[46] demonstrated that xanthomicrol can relax gastrointestinal smooth muscle.

DOI: 10.1021/np500671v
J. Nat. Prod. XXXX, XXX, XXX−XXX

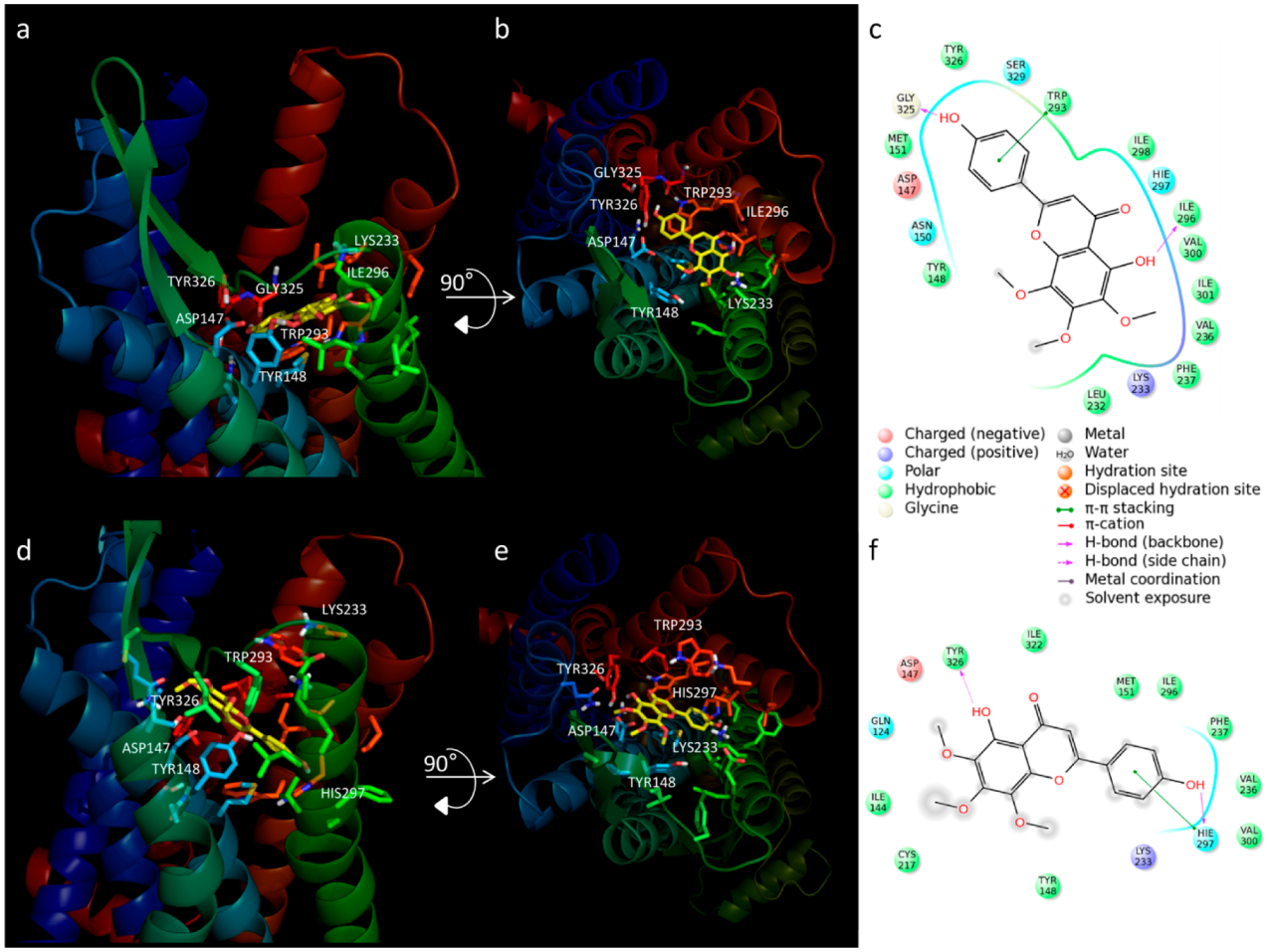

Figure 5. Putative binding modes of compound **1** in complex with MOR. Front view: within the membrane plane, extracellular side (a) and intracellular side (d); (b, e) view from the top of the channel; (c, f) 2D depictions of interactions of the ligand with MOR.

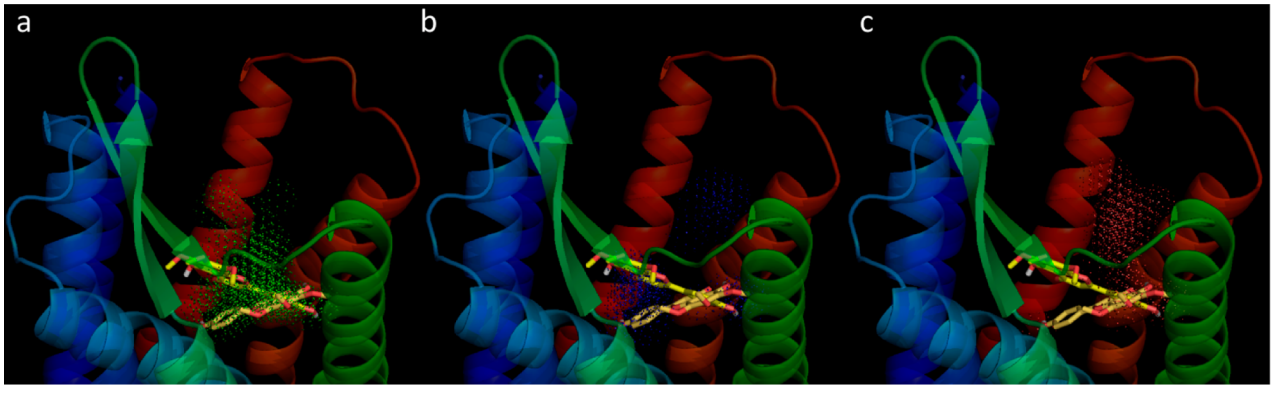

Figure 6. Visualization of GRID maps together with the two conformations of compound **1** obtained by docking experiments: (a) in green, DRY probe (hydrophobic), (b) in blue, N1 probe (donor), and (c) in red, O probe (acceptor).

In summary, the data indicate that xanthomicrol represents a valuable structure for further development into a potential MOR antagonist. Opioid antagonists have been approved for alcohol dependence[47] and are efficacious in treating mental pathologies such as gambling disorder.[48] Further studies are currently under way to evaluate if other systems, such as serotonergic, dopaminergic, and cholinergic, are involved in the mechanism of action of xanthomicrol. Biological and structural information as well as SAR data will directly lead to the optimization and generation of a focused library of analogous natural compounds with appropriate prerequisites.

EXPERIMENTAL SECTION

General Experimental Procedures. Optical rotations were measured in $CHCl_3$ at 25 °C using a PerkinElmer 241 polarimeter. UV spectra were recorded on a GBC Cintra 5 spectrophotometer. IR spectra were performed with a PerkinElmer system 2000 FT-IR spectrophotometer using KBr mulls. NMR spectra were recorded at 25 °C on a Unity Inova 500NB high-resolution spectrometer (Agilent Technologies, CA, USA) operating at 500 MHz for ^{1}H and 100 MHz for

DOI: 10.1021/np500671v
J. Nat. Prod. XXXX, XXX, XXX−XXX

^{13}C, respectively. All spectra were measured at 25 °C in $CDCl_3$ and referenced against residual $CHCl_3$ in $CDCl_3$ (^1H 7.27 ppm) and $CDCl_3$ (^{13}C 77.0 ppm). HR-ESIMS (positive mode) were measured on an Agilent 6520 time of flight (TOF) MS instrument, while ESIMS experiments were performed on a Varian 1200 L triple quadrupole. Column chromatography was carried out under TLC monitoring using silica gel (40−63 μm, Merck) and Sephadex LH-20 (25−100 μm, Pharmacia). For VLC, silica gel (40−63 μm) (Merck) was used. TLC was performed on silica gel 60 F_{254} or RP-18 F_{254} (Merck). For molecular modeling, the PC Spartan Pro software program (Wavefunction Inc.) was used.

Plant Material. *Stachys glutinosa* aerial parts were collected in April 2006 at Capoterra, Sardinia, Italy. The plant material was identified by Dr. Marco Leonti (University of Cagliari, Department of Biomedical Sciences). A voucher specimen (No. 0425) was deposited in the Herbarium of the Department of Life and Environmental Science, Drug Sciences Section, University of Cagliari.

Extraction and Isolation. Air-dried and powdered aerial parts of *S. glutinosa* (547.8 g) were ground and extracted with CH_2Cl_2 (5 L) by percolation at room temperature to give 52.42 g of dried extract. An aliquot (20 g) of the CH_2Cl_2 extract was subjected to VLC (silica gel, 150 g, 40−63 μm) using a step gradient of *n*-hexane/CH_2Cl_2/EtOAc/MeOH (7.5:2.5:0:0 to 0:0:7.5:2.5, 500 mL each) to yield eight main fractions (F1−F8). Fraction F3 (1.13 g, eluted with CH_2Cl_2, 500 mL) was separated by column chromatography (CC) over silica gel using CH_2Cl_2/MeOH (9.9:0.1) as eluent to obtain compound **3** (12.0 mg). An aliquot (0.5 g) of fraction F4 (3.06 g) eluted with CH_2Cl_2/EtOAc (7.5:2.5) was purified by CC over Sephadex LH-20 using MeOH as eluent, giving five subfractions (F4.1−F4.5). F4.3 (230 mg) was further chromatographed over Sephadex LH-20 to obtain four subfractions (F4.3.1−F4.3.4). F4.3.3 (44.5 mg) was purified by solid-phase extraction (SPE) (RP-18) using acetonitrile/H_2O (7:3) as eluent to give compound **4** (15.2 mg). F5 (0.91 g) was treated with EtOAc to give a solid and a solution. The solid was filtered off and purified by Sephadex LH-20 (MeOH) to give compound **1** (404.4 mg). F6 (0.70 g) was subjected to CC (silica gel) using *n*-hexane/EtOAc (6.5:3.5) as eluent to obtain **8** (47.7 mg). F8 (1.48 g) was chromatographed on silica gel using CH_2Cl_2/MeOH (9.9:0.1) as eluent to give five subfractions (F8.1−F8.5). F8.3 (145.3 mg) was purified by Sephadex LH-20 (MeOH) to give **2** (15.0 mg) and **7** (40 mg).

3α,4α-Epoxyroseostachenol (7): white, amorphous solid $[\alpha]^{25}_D$ +19.4 (*c* 0.07, CH_2Cl_2); ^1H NMR ($CDCl_3$, 500 MHz) δ 5.88 (1H, dd, *J* = 11.0, 17.5 Hz, H-14), 5.21 (1H, dd, *J* = 1.0, 17.2 Hz, H-15 trans), 5.08 (1H, dd, *J* = 1.0, 10.8 Hz, H-15 cis), 3.90 (1H, ddd, *J* = 2.0, 6.0 Hz, H-2), 3.06 (1H, br s, H-3), 1.65 (1H, m, H-6β), 1.63 (1H, m, H-1β), 1.45 (2H, m, H-7), 1.42 (1H, m, H-8), 1.37 (1H, m, H-12β), 1.36 (1H, m, H-11β), 1.25 (1H, m, H-6α), 1.24 (1H, m, H-11α), 1.23 (1H, m, H-12α), 1.20 (3H, s, H-18), 1.16 (1H, m, H-1α), 1.04 (3H, s, H-19), 0.88 (1H, br, d, *J* = 11.5 Hz, H-10), 0.76 (3H, d, *J* = 6.5 Hz, H-17), 0.66 (3H, s, H-20); ^{13}C NMR ($CDCl_3$, 100 MHz) δ 144.9 (CH, C-14), 112.0 (CH_2, C-15), 73.3 (C, C-13), 70.7 (CH, C-2), 70.4 (C, C-4), 65.2 (CH, C-3), 46.3 (CH, C-10), 38.6 (C, C-9), 36.8 (CH_2, C-6), 36.2 (C, C-5), 35.8 (CH, C-8), 35.3 (CH_2, C-12), 31.8 (CH_2, C-11), 27.9 (CH_2, C-7), 27.8 (CH_3, H-16), 25.3 (CH_2, H-1), 19.4 (CH_3, H-18), 18.7 (CH_3, H-20), 16.5 (CH_3, H-19), 15.8 (CH_3, H-17); HRTOFESIMS (*m*/*z*) 345.2418 $[M + Na]^+$ (calcd for $C_{20}H_{34}O_3$ 345.2406).

Semisynthesis of 5-Demethyltangeretin (5). A mixture of xanthomicrol (**1**) (50.0 mg, 0.1453 mmol) and K_2CO_3 (1.2 equiv, 24.1 mg) in a mixture of acetone/CH_2Cl_2 (1:1, 8 mL) was added to Me_2SO_4 (16.5 μL, 0.1744 mmol), and the reaction mixture then refluxed for 4 h. The resulting solution was cooled and Na_2CO_3 (25 mL, 10%) was added. The solution was extracted with CH_2Cl_2 (3 × 10 mL). The organic layer was concentrated under vacuum, and the methylated derivative was subsequently purified over silica gel using MeOH/CH_2Cl_2 (9.9:0.1) to give **5** (23.2 mg, 44.6%) as a white solid: mp 172−173 °C (*n*-hexane); spectroscopic data (UV, MS, NMR) identical to those reported in the literature.[24]

Semisynthesis of Tangeretin (6). To a mixture of xanthomicrol (**1**) (65.9 mg, 0.1916 mmol) and K_2CO_3 (2.5 equiv, 66.2 mg, in a mixture of acetone/CH_2Cl_2 (1:1, 10 mL)) was added Me_2SO_4 (45.3 μL, 0.479 mmol), and then the reaction mixture was refluxed for 4 h. The resulting solution was cooled and Na_2CO_3 (35 mL, 10%) added. The solution was extracted with CH_2Cl_2 (3 × 10 mL). The organic layer was concentrated under vacuum, and the residue was subsequently purified over Sephadex LH-20 (MeOH) to give **5** (21.8 mg, 31.8%) and **6** (5.4 mg, 8%). Tangeretin (**6**) was obtained in 8% yield as a white solid: mp 151−152 °C (*n*-hexane); spectroscopic data (UV, MS, NMR) identical to those reported in the literature.[10,25]

Animals. Male CD1 mice (Charles River, Calco, Italy, 20−25 g) were used for both receptor binding and behavioral studies. Animals were housed in an animal facility on a 12 h light/dark cycle (lights on from 07:00 A.M.), at a constant room temperature of 21 ± 1 °C (relative humidity approximately 60%). Standard rodent chow and water were available ad libitum. Animals were allowed to adapt to the animal facility conditions for at least 2 weeks after arrival. Procedures involving animals and their care were conducted in accordance with the institutional guidelines that are in compliance with national (D.L. 116/1992) and international laws and policies (EEC Council Directive 86/609, OJL 358, 1, Dec 12, 1987; Guide for the Care and Use of Laboratory Animals, U.S. National Research Council, 1996) and were approved by the Institutional Animal Ethics Committee of University of Cagliari, Italy (No. 135/2013 B). Every effort was made to minimize animal pain and discomfort and to reduce the number of experimental subjects.

Drugs and Chemicals. In radioligand binding assays compounds were dissolved in dimethyl sulfoxide (DMSO, Sigma-Aldrich, Milan, Italy). [^3H]-DAMGO ([D-Ala2, N-Me-Phe4,Gly-ol5]-enkephalin) and [^3H]-DPDPE ([D-Pen^2, D-Pen^5]-enkephalin) were purchased from PerkinElmer, Monza (MB), Italy. Naloxone was obtained from Tocris Cookson Ltd. (Bristol, UK). In the behavioral study, morphine hydrochloride (Salars, Como, Italy) was dissolved in saline (NaCl 0.9%) and administered subcutaneously (sc) in a volume of 5 mL/kg. Xanthomicrol was suspended in saline with DMSO (1%) and a few drops of Tween 80 and administered intraperitonealy (ip) in a volume of 5 mL/kg.

Receptor Binding Experiments: [^3H]-DAMGO−[^3H]-DPDPE (Opioid Receptors) Binding Assay. Ligand binding assays were carried out according to the procedure described by Ruiu et al.[49] Briefly, the whole brain minus the cerebellum was homogenized with Polytron in 50 volumes (w/v) of 50 mM Tris-HCl (pH 7.4), centrifuged at 48000*g* for 20 min at 4 °C, resuspended in 50 volumes of the same buffer solution, and incubated at 37 °C for 45 min. After a further centrifugation step at 48000*g* for 20 min at 4 °C, the final pellet was resuspended in the same buffer solution. Brain membranes (150−200 μg of protein) were incubated with the appropriate concentration of [^3H]-DAMGO or [^3H]-DPDPE in Tris-HCl buffer at 25 °C for 60 min in the absence or presence of naloxone (1 μM). The binding reaction was stopped by rapid filtration under vacuum through glass-fiber filters (Whatman GF/B) using a Brandell 36-sample harvester (Gaithesburg, MD, USA), and thereafter the filters were washed with 4 × 5 mL of ice-cold 50 mM Tris-HCl buffer (pH 7.4). The affinity of compounds **1**−**8** was compared with that of the reference compound morphine hydrochloride (MOR K_i = 1.2 ± 0.03 nM; DOR K_i = 100 ± 12 nM).

Analysis of Samples. Displacement curves were carried out using serial dilutions ranging from 2 to 0.001 mg/mL of the CH_2Cl_2 extract and from 100 to 0.001 μM of all other compounds. To avoid possible undesired effects on radioligand binding, DMSO concentration in the different assays never exceeded 1% (v/v). Filter-bound radioactivity was counted in a liquid scintillation counter (Tricarb 2900; PerkinElmer Life Sciences, Boston, MA, USA) using Ultima Gold (Packard, USA) as scintillation fluid. Protein content was determined using the Bio-Rad Dc Kit (Bio-Rad Laboratories GmbH, Munich, Germany) following the manufacturer's instructions.

Tail-Flick Test. The antinociceptive effects were quantified using the tail-flick test.[50] An automated device (model 7360, Ugo Basile, Italy) was used to determine the tail-flick latency, defined by the time (s) at which the animals withdraw the tail from a radiant heat source. Mice were held and gently restrained above the apparatus; the light beam was focused 1.5 cm from the tip of the ventral surface of the tail. The stimulus intensity was adjusted to result in a mean predrug control latency of 2−3 s, and a cutoff time of 12 s was applied to avoid tissue damage. Mice were

DOI: 10.1021/np500671v
J. Nat. Prod. XXXX, XXX, XXX−XXX

pretreated with saline or xanthomicrol (40 and 80 mg/kg) 30 min before saline or morphine (5 mg/kg) treatment. Basal algesia was assessed right before saline or xanthomicrol pretreatment (baseline). The effects of the drugs were evaluated 30, 60, and 120 min after morphine treatment.

Data Analysis. Data from radioligand inhibition experiments were analyzed by nonlinear regression analysis of a Sigmoid Curve using the GraphPad Prism program (Graph Pad Software, Inc., San Diego, CA, USA). IC_{50} values were derived from the calculated curves and converted to K_i values as described previously.[51] All receptor binding experiments were performed in triplicate, and results were confirmed in at least four independent experiments. Treatment-induced variations in tail-flick response were calculated as the percentage of maximal possible effect (MPE) according to the following formula: MPE [%]: $[(T_1 - T_0)/(T_2 - T_0)] \times 100$, where T_0 and T_1 are the latency before (baseline) and after treatment, and T_2 is the cutoff time (12 s). Behavioral data were expressed as mean ± standard error (SEM) of %MPE and were analyzed separately by repeated measure three-way analysis of variance (ANOVA) with pretreatment (saline and xanthomicrol) and treatment (saline and morphine) as between-subjects factors and time as within-subjects factor (repeated measures). When appropriate, post hoc comparisons were done using Tukey's test.

Molecular Modeling. The ligand was docked in the global minimum energy conformation as determined by molecular mechanics conformational analysis performed with Macromodel software.[52] Theoretical 3D models of the most active compound were built by means of Maestro GUI. The molecule was then submitted to a conformational search of 1000 steps with an energy window for saving structures of 10 kJ/mol. The algorithm used was the Monte Carlo method with MMFFs (Merck molecular force fields)[53] followed by an energy minimization carried out using the MMFFs, the GB/SA[54] water implicit solvation model, and the Polak−Ribier conjugate gradient (PRCG) method for 5000 iterations, converging on gradients with a threshold of 0.05 kJ(mol·Å)$^{-1}$.

The protein structure was obtained from the PDB Web site.[32] It was prepared by the Protein Preparation Wizard protocol.[55] Missing side chains were added and optimized.

Molecular docking calculations were performed using FLAPdock, Glide, Autodock, and Vina programs. FLAPdock[27,28] was applied since we have already noticed its high performance in docking experiments (unpublished data). In this work, the "best" setting was applied since it resulted in being slightly better than the "fast". Several settings and protocols were applied using the Glide program (GlideSP-XP, IFD, QMPL).[26,55−58] Glide SP with default settings was the best. Instead for Autodock[29] all setting were left as default except for the higher number of energy evaluations, to ensure a sufficient sampling of the conformational space of the ligands (5M), and 100 runs since better redocking results were obtained. Finally, with Vina[30] default settings were applied: the increased value of exhaustiveness did not improve the RMSD of redocking results.

Best settings reproducing the experimental binding mode of FNA were applied to dock xanthomicrol. Then, in order to take into account the induced fit mechanism, the resulting top ranked theoretical complexes were subject to 10 000 steps of the PRCG energy minimization method using the AMBER* force field. The residues, located in a radius of 5 Å around the ligand, were left free to move. The optimization process was performed up to the derivative convergence criterion equal to 0.01 kJ/(mol·Å)$^{-1}$. Depictions were taken by means of Pymol[59] and Maestro GUI.[55]

■ ASSOCIATED CONTENT

Ⓢ Supporting Information

NMR and HRESIMS spectra of compound 7. This material is available free of charge via the Internet at http://pubs.acs.org.

■ AUTHOR INFORMATION

Corresponding Author

*Tel: + 39-706758979. Fax: + 39-706758553. E-mail: cottiglf@unica.it.

Author Contributions

[▽]S. Ruiu and N. Anzani contributed equally.

Notes

The authors declare no competing financial interest.

■ ACKNOWLEDGMENTS

We are thankful to Dr. M. Leonti (Department of Biomedical Sciences) for identification of the plant material. This work was partially supported by Fondazione Banco di Sardegna (Sassari, Italy; Prot. N. U680.2013/AI.604.MGB) and by Interregional Research Center for Food Safety and Health at the Magna Græcia University of Catanzaro (MIUR PONa3 00359).

■ REFERENCES

(1) Verma, A. K.; Pratap, R. *Nat. Prod. Rep.* **2010**, *27*, 1571−1593.
(2) Crozier, A.; Jaganath, I. B.; Clifford, M. N. *Nat. Prod. Rep.* **2009**, *26*, 1001−1043.
(3) Walgren, R. A.; Walle, U. K.; Walle, T. *Biochem. Pharmacol.* **1998**, *55*, 1721−1727.
(4) Walle, T.; Otake, Y.; Brubaker, J. A.; Walle, U. K.; Halushka, P. V. *Br. J. Clin. Pharmacol.* **2001**, *51*, 143−146.
(5) Chen, A. Y.; Chen, C. Y. *Food Chem.* **2013**, *138*, 2099−2107.
(6) Walle, T. *Mol. Pharmaceutics* **2007**, *4*, 826−832.
(7) Manach, C.; Donovan, J. L. *Free Radical Res.* **2004**, *38*, 771−785.
(8) Wen, X.; Walle, T. *Drug Metab. Dispos.* **2006**, *34*, 1786−1792.
(9) Mizuno, M.; Iinuma, M.; Ohara, M.; Tanaka, T.; Iwamasa, M. *Chem. Pharm. Bull.* **1991**, *39*, 945−949.
(10) Li, S.; Lo, C.-Y.; Ho, C.-T. *J. Agric. Food Chem.* **2006**, *54*, 4176−4185.
(11) Dandan, W.; Jian, W.; Xuehui, H.; Ying, Y.; Kunyi, N. *J. Pharm. Biomed. Anal.* **2007**, *44*, 63−69.
(12) Ahmad, F.; Bakar, S. A.; Ibrahim, A. Z.; Read, R. W. *Planta Med.* **1997**, *63*, 193−194.
(13) Hernández, I. M.; Cuesta-Rubio, O.; Fernández, M. C.; Pérez, A. R.; Montes de Oca Porto, R.; Piccinelli, A. L.; Rastrelli, L. *J. Agric. Food Chem.* **2010**, *58*, 4725−4730.
(14) Ruiu, S.; Anzani, N.; Orrù, A.; Floris, C.; Caboni, P.; Maccioni, E.; Distinto, S.; Alcaro, S.; Cottiglia, F. *Bioorg. Med. Chem.* **2013**, *21*, 7074−7082.
(15) Pignatti, S. *Flora d'Italia*; Edagricole: Bologna, 1982; Vol. *II*, p 468.
(16) Atzei, A. *Le Piante Nella Tradizione Popolare della Sardegna*; Delfino: Sassari, 2003; p 244.
(17) Camarda, I.; Valsecchi, F. *Piccoli Arbusti Liane e Suffrutici Spontanei della Sardegna*; Delfino: Sassari, 1992; p 205.
(18) Manabe, S.; Nishino, C. *Tetrahedron* **1986**, *42*, 3461−3470.
(19) Jahaniani, F.; Ebrahimi, S. A.; Rahbar-Roshandel, N.; Mahmoudian, M. *Phytochemistry* **2005**, *66*, 1581−1592.
(20) Kuhnt, M.; Rimpler, H.; Heinrich, M. *Phytochemistry* **1994**, *36*, 485−489.
(21) Oshitari, T.; Okuyama, Y.; Miyata, Y.; Kosano, H.; Takahashi, H.; Natsugari, H. *Bioorg. Med. Chem.* **2011**, *19*, 7085−7092.
(22) Agrawal, P. K. *Carbon−13 NMR of Flavonoids*; Elsevier: Amsterdam, 1989; p 154.
(23) Fazio, C.; Passannanti, S.; Paternostro, M. P.; Piozzi, F. *Phytochemistry* **1992**, *31*, 3147−3149.
(24) Morimoto, M.; Kumeda, S.; Komai, K. *J. Agric. Food Chem.* **2000**, *48*, 1888−1891.
(25) Iinuma, M.; Matsuura, S.; Kusuda, K. *Chem. Pharm. Bull.* **1980**, *28*, 708−716.
(26) Friesner, R. A.; Murphy, R. B.; Repasky, M. P.; Frye, L. L.; Greenwood, J. R.; Halgren, T. A.; Sanschagrin, P. C.; Mainz, D. T. *J. Med. Chem.* **2006**, *49*, 6177−6196.
(27) *FLAPdock*; Molecular Discovery Ltd.: London, UK (http://www.moldiscovery.com).

DOI: 10.1021/np500671v
J. Nat. Prod. XXXX, XXX, XXX−XXX

(28) Artese, A.; Cross, S.; Costa, G.; Distinto, S.; Parrotta, L.; Alcaro, S.; Ortuso, F.; Cruciani, G. *Wiley Interdiscip. Rev.: Comp. Mol. Sci.* **2013**, *3*, 594−613.
(29) Morris, G. M.; Goodsell, D. S.; Halliday, R. S.; Huey, R.; Hart, W. E.; Belew, R. K.; Olson, A. J. *J. Comput. Chem.* **1998**, *19*, 1639−1662.
(30) Trott, O.; Olson, A. J. *J. Comput. Chem.* **2010**, *31*, 455−461.
(31) Wolf, A.; Zimmermann, M.; Hofmann-Apitius, M. *J. Chem. Inf. Model.* **2007**, *47*, 1036−1044.
(32) Manglik, A.; Kruse, A. C.; Kobilka, T. S.; Thian, F. S.; Mathiesen, J. M.; Sunahara, R. K.; Pardo, L.; Weis, W. I.; Kobilka, B. K.; Granier, S. *Nature* **2012**, *485*, 321−326.
(33) Coleman, R. S.; Woodward, R. L.; Hayes, A. M.; Crane, E. A.; Artese, A.; Ortuso, F.; Alcaro, S. *Org. Lett.* **2007**, *9*, 1891−1894.
(34) Emsley, P.; Cowtan, K. *Acta Crystallogr., Sect D: Biol. Crystallogr.* **2004**, *60*, 2126−2132.
(35) Goodford, P. J. *J. Med. Chem.* **1985**, *28*, 849−857.
(36) Higgs, J.; Wasowski, C.; Loscalzo, L. M.; Marder, M. *Neuropharmacology* **2013**, *72*, 9−19.
(37) Webster, D. E.; He, Y.; Chen, S.-N.; Pauli, G. F.; Farnsworth, N. R.; Wang, Z. J. *Biochem. Pharmacol.* **2011**, *81*, 170−177.
(38) Lovell, K. M.; Simpson, D. S.; Christopher, W.; Cunningham, C. W.; Prisinzano, T. E. *Future Med. Chem.* **2009**, *1*, 285−301.
(39) Katavic, P. L.; Lamb, K.; Navarro, H.; Prisinzano, T. E. *J. Nat. Prod.* **2007**, *70*, 1278−1282.
(40) Butterweck, V.; Nahrstedt, A.; Hufeisen, J. E. S.; Rauser, L.; Popadak, J. S. B.; Ernsberger, P.; Roth, B. L. *Psycopharmacology* **2002**, *162*, 193−202.
(41) Pinheiro, M. M. G.; Boylan, F.; Fernandes, P. D. *Life Sci.* **2012**, *91*, 293−300.
(42) Özkay, Ü. D.; Can, Ö. D. *Pharmacol., Biochem. Behav.* **2013**, *109*, 23−30.
(43) Vidyalakshmi, K.; Kamalakannan, P.; Viswanathan, S.; Ramaswamy, S. *Pharmacol., Biochem. Behav.* **2010**, *96*, 1−6.
(44) Anjaneyulu, M.; Chopra, K. *Prog. Neuropsychopharmacol. Biol. Psychiatry* **2003**, *27*, 1001−1005.
(45) Moghaddam, G.; Ebrahimi, S. A.; Rahbar-Roshandel, N.; Foroumadi, A. *Phytother. Res.* **2012**, *26*, 1023−1028.
(46) Meckes, M.; Calzada, F.; Paz, D.; Rodríguez, J.; Ponce-Monter, H. *Planta Med.* **2002**, *68*, 467−468.
(47) Nutt, D. J. *J. Psychopharmacol.* **2014**, *28*, 8−22.
(48) Łabuzek, K.; Beil, S.; Beil-Gawełczyk, J.; Gabryel, B.; Franic, G.; Okopień, B. *Pharmacol. Rep.* **2014**, *66*, 811−820.
(49) Ruiu, S.; Longoni, R.; Spina, L.; Orrù, A.; Cottiglia, F.; Collu, M.; Kasture, S.; Acquas, E. *Behav. Pharmacol.* **2013**, *24*, 133−143.
(50) Orrù, A.; Marchese, G.; Casu, G.; Casu, M. A.; Kasture, S.; Cottiglia, F.; Acquas, E.; Mascia, M. P.; Anzani, N.; Ruiu, S. *Phytomedicine* **2014**, *21*, 745−752.
(51) Cheng, Y. C.; Prusoff, W. H. *Biochem. Pharmacol.* **1973**, *22*, 3099−3108.
(52) Mohamadi, F.; Richards, N. G. J.; Guida, W. C.; Liskamp, R.; Lipton, M.; Caufield, C.; Chang, G.; Hendrickson, T.; Still, W. C. *J. Comput. Chem.* **1990**, *11*, 440−467.
(53) Halgren, T. *J. Comput. Chem.* **1996**, *17*, 520−552.
(54) Hasel, W.; Hendrickson, T. F.; Still, W. C. *Tetrahedron Comput. Methodol.* **1988**, *1*, 103−116.
(55) *Maestro GUI, Schrodinger Suite*; Schrödinger LLC.: New York, NY, USA, 2014.
(56) Friesner, R. A.; Murphy, R. B.; Repasky, M. P.; Frye, L. L.; Greenwood, J. R.; Halgren, T. A.; Sanschagrin, P. C.; Mainz, D. T. *J. Med. Chem.* **2006**, *49*, 6177−6196.
(57) Chung, J. Y.; Hah, J.-M.; Cho, A. E. *J. Chem. Inf. Model.* **2009**, *49*, 2382−2387.
(58) Sherman, W.; Day, T.; Jacobson, M. P.; Friesner, R. A.; Farid, R. *J. Med. Chem.* **2006**, *49*, 534−553.
(59) *PyMOL Molecular Graphics System*, Version 1.5.0.4; Schrödinger, LLC, 2010.

DOI: 10.1021/np500671v
J. Nat. Prod. XXXX, XXX, XXX−XXX